

# The demonstration of conformal maps with two-dimensional foams

W Drenckhan, D Weaire and S J Cox

Department of Physics, Trinity College, Dublin 2, Republic of Ireland

Received 14 August 2003

Published 25 March 2004

Online at [stacks.iop.org/EJP/25/429](http://stacks.iop.org/EJP/25/429) (DOI: 10.1088/0143-0807/25/3/010)

## Abstract

Monodisperse two-dimensional foams are produced by trapping a layer of equal-volume bubbles between two glass surfaces. The application of an appropriately angled or curved surface imposes a specific variation of the bubble area with position in the foam. With this easily demonstrated technique the foam can be created in such a way as to reproduce conformal maps of the hexagonal honeycomb lattice to a good approximation.

## 1. Introduction

Conformal mapping finds uses in many areas of physics where two-dimensional (2D) fields or patterns are found. Such a mapping can be constructed using any analytic function  $w = f(z)$ , according to

$$u + iv = f(x + iy),$$

where  $z = x + iy$  and  $w = u + iv$ . One of its principal properties is *isogonality*: any two curves that intersect are transformed into curves that intersect *at the same angle*. The application of conformal maps is perhaps most familiar in the context of 2D incompressible fluid mechanics (Prandtl and Tietjens 1934), where they are used to produce equivalent problems with simpler boundary conditions.

Certain patterns that occur naturally are immediately recognizable as conformal transformations of simpler ones. Popular examples include cellular growth patterns in biology (Weaire and Rivier 1984), structures formed by magnetized steel balls in external force fields (Rothen *et al* 1993, Rothen and Pierański 1996), ferrofluid foams in magnetic fields (Elias *et al* 1999) or crystal growth in amorphous films (Kolosov 1995).

In our studies of 2D foams we have encountered another case in a particularly accessible experimental system that has the merit of being very easily understood. We find that 2D foam patterns with a specified variation of bubble area can be considered as conformal transformations of the hexagonal (honeycomb) structure (see figure 1), which minimizes the line length (or energy) of a 2D foam with cells of equal area (Hales 2001). Isogonality upon transformation preserves a very important property of any 2D foam at equilibrium: in order

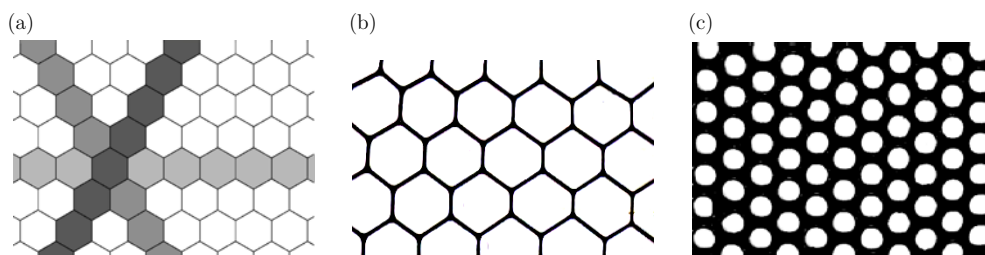


**Figure 1.** Examples of the *honeycomb* structure, the 2D monodisperse foam with minimum energy, used as the initial pattern for the conformal transformations. (a) Computational pattern. The pattern of shading will be retained in the transformed structures to aid visualization. Experimentally obtained (b) dry and (c) wet 2D monodisperse foams sandwiched between two parallel glass plates.

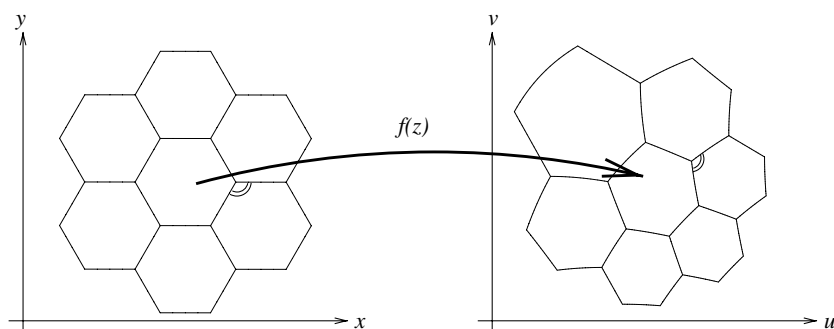


**Figure 2.** A conformal mapping of a hexagonal ‘bubble’ preserves the angles at vertices, but not the area of each bubble. Only *bilinear* maps transform arcs of circles into arcs of circles.

to balance surface tension, edges have to meet three-fold at  $120^\circ$  (Plateau 1873). Another property is only preserved by the special class of *bilinear* conformal maps: that all edges have to be arcs of circles whose curvatures add to give zero at every vertex (see section 2.2). Together these conditions guarantee that the new structure obeys the rules of equilibrium. For the general case, the theoretically mapped patterns will only be approximations to the experimentally observed equilibrium structures.

In the following section, we review some properties of conformal maps before showing how certain examples can be realized with a simple setup.

## 2. Conformal maps, inversion and soap froth

Locally, a conformal mapping  $f(z)$  preserves angles (the isogonal property) but not areas (see figure 2). If  $ds_z = (dx^2 + dy^2)^{\frac{1}{2}}$  is a small element of line in the  $(x, y)$  plane, it will be magnified according to

$$ds_w = \left| \frac{dw}{dz} \right| ds_z = |f'(z)| ds_z \quad (1)$$

upon transformation. Hence a small element of area will be scaled by a factor of  $|f'(z)|^2$ . It is this change of area we seek to reproduce experimentally.

We will concentrate on two types of maps of the hexagonal lattice, which are characterized by their symmetry properties and are of particular relevance to many areas of science:

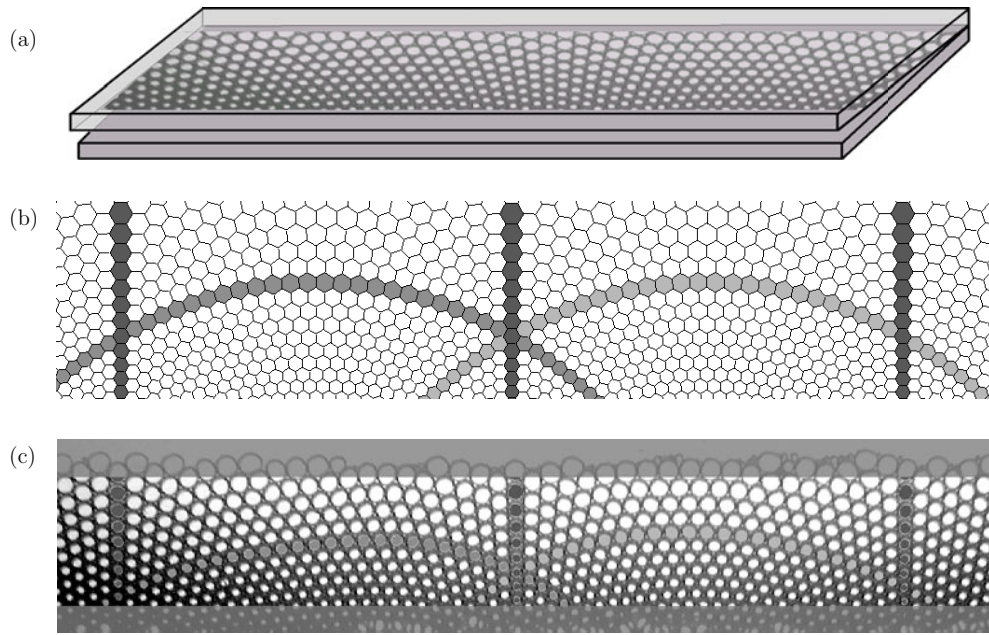


**Figure 3.** The logarithmic map (gravity's rainbow). (a) Experimental setup. The bottom plate is horizontal. (b) Numerical mapping of a perfect honeycomb using equation (2). (c) Experimentally obtained pattern. The shading shows how lines of neighbouring cells that were initially straight (compare figure 1) are transformed.

- Conformal transformations with translational symmetry (section 2.1).
- Conformal transformations with rotational symmetry (section 2.2).

For a more detailed description of the numerical mapping procedure refer to the appendix.

### 2.1. Conformal transformations with translational symmetry

It can be shown that the *logarithmic* map is the *only* conformal transformation with translational symmetry (Rothen *et al* 1993). It is

$$w = f(z) = u(z) + iv(z) = (i\alpha)^{-1} \log(i\alpha z), \quad (2)$$

which maps the exterior of a circle of radius  $\alpha$  onto the upper half plane. For an example of the effect of this upon the honeycomb structure, see figure 3(b). This elegant pattern has been dubbed ‘gravity’s rainbow’ (Pierański 1989). It has a translational period of  $2\pi/\alpha$ .

Application of equation (1) reveals that the area  $A$  of the transformed hexagons depends only on  $v$ :

$$A(w) = A(v) \sim e^{2\alpha v}. \quad (3)$$

### 2.2. Conformal transformations with radial symmetry

Any conformal map of radial symmetry has to satisfy the differential equation (Rothen *et al* 1993)

$$w^{-\delta} dw = \beta dz, \quad (4)$$

where  $\delta$  is a real and  $\beta$  a complex number. Equation (4) has two different solutions depending on the value of  $\delta$ .

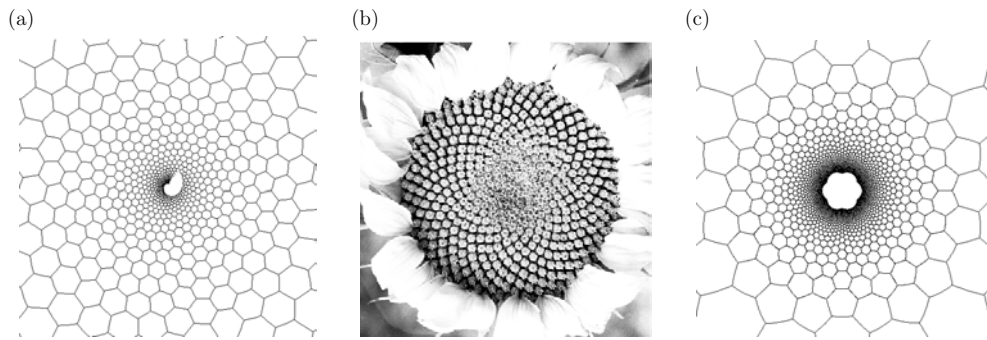


**Figure 4.** Two special cases of maps with radial symmetry. (a) Numerical example of phyllotaxis using equation (5). (b) Phyllotactic design shown by a sunflower (photograph taken by Yves Couder). (c) Numerical example of the inversion defined by equation (8) with  $\delta = 2$ .

For  $\delta = 1$  we obtain the map

$$w = f(z) = w_0 e^{\beta z}, \quad (5)$$

which is commonly referred to as *phyllotaxis* (Jean 1984) and found in many systems governed by cellular growth. Popular examples are the florets of a sunflower (figure 4(b)) or the scales of a pineapple (Atela *et al* 2003). The latter type of cylindrical phyllotaxis can be beautifully reproduced using the regular stacking of soap bubbles in cylindrical tubes (Weaire *et al* 1992).

The case  $\delta \neq 1$  is more general and we will refer to it as the *circle map*:

$$w = f(z) = w_0 z^{1/(1-\delta)}. \quad (6)$$

The area  $A$  of the transformed hexagons varies with distance  $r$  from the centre as

$$A(w) = A(r) \sim r^{2\delta}. \quad (7)$$

The circle map also contains the important special case of *inversion* for  $\delta = 2$  (see figure 4(c)):

$$f(z) = z^{-1}, \quad (8)$$

or more generally the bilinear or *homographic* transformation generated by

$$f(z) = (az + b)/(cz + d).$$

This combines the inversion with an arbitrary translation and rotation, which are of no significance in the present context. This case has additional special properties that are of particular relevance to 2D soap froths, as noted by Weaire (1999). Under inversion, arcs of circles remain circular upon transformation. They conform to a further property which may be obliquely stated as follows: any 2D soap froth structure in static equilibrium transforms into another equilibrium structure. This requires rather more than the preservation of  $120^\circ$  angles at vertices. The existence of a unique gas pressure in each cell requires that the curvatures of cell edges (related to pressure differences by the Laplace law) add to give zero at every vertex. This zero sum rule is preserved upon inversion (Weaire 1999).

Only an inversion has this *exact* property of preserving equilibrium for the 2D soap froth while changing the area of its constituent bubbles. However, a general conformal transformation can achieve a *good approximation* to this property. To see this, note that any  $f(z)$  can be approximated by an inversion (or homographic transformation) in the neighbourhood of a point  $z_0$ , in the sense that terms in its Taylor expansion in  $z - z_0$  are

identical up to second order. This is a sufficient condition to allow us to assume that the conformal transformation has similar effects on local curvatures to those of the bilinear transformation which approximates it. But in general this holds only to lowest order, so the sum rule holds at every vertex, but the curvature varies along each edge.

Such arguments can be adduced to transform *any* equilibrium soap froth structure.

### 3. Experimental procedure and simulation

Experimentally, 2D foams are produced by squeezing one layer of bubbles between two glass plates, between a glass plate and a liquid surface, or by collecting bubbles in one layer on a liquid surface (the *Bragg raft*). Many such froths have been analysed in the past, following the lead of Bragg and Nye (1947) and Smith (1952).

In our experiment, bubbles of equal volume are generated by blowing nitrogen at constant pressure through a nozzle into a surfactant solution (we use tap water and Fairy liquid). Glycerol is added to the solution to prolong the lifetime of the foam. The bubbles are then trapped between two glass surfaces. A variation of the apparent 2D bubble area with position within the pattern can be imposed by using a curved upper surface. If the separation between the surface shapes is  $d(w)$ , then the area of a bubble varies as  $A(w) \sim d(w)^{-1}$ . The precise shapes of surfaces required by theory are difficult to make, but fortunately we find that astonishingly good results can be obtained by using small bubbles and much simpler surfaces, which can be considered as approximations of the required ones (see the next section for details). The number of available geometries is plentiful: inclined plates or cylinders for the map with translational symmetry, spheres of different radii and funnels of different shapes for maps with radial symmetry. We will concentrate on a small selection.

Even if the computed structures of the previous section are the ideal, energy-minimizing ones (and we make no claim to prove this), they do not occur spontaneously in this procedure. A many-bubble foam has a vast energy landscape of meta-stable states, which need to be avoided by an annealing-like experimental procedure. This involves keeping the foam very wet and varying the spacing and angles between the surfaces repeatedly. After a while, the perfect pattern begins to emerge and one can concentrate on eliminating isolated defects, which glide beautifully along the arches of the pattern.

#### 3.1. Conformal 2D foam with translational symmetry

To obtain gravity's rainbow defined in section 2.1, we should introduce an upper plate which decreases exponentially in height in one direction,  $d(w) \sim e^{-2\alpha v}$ . However, we obtain an excellent approximation to this map with a linear decrease, corresponding to a tilt of the upper plate. The setup is shown in figure 3(a). A large cluster of bubbles is produced in order to reduce any quantizing influence of the boundaries of the specimen cluster on the periodic pattern—the boundaries are so far away that they have only a negligible influence on the choice of period. Using a large cylinder instead of the slanted upper plate works equally well. Figure 3(c) shows an experimental result obtained by projecting the foam with an ordinary overhead projector.

The similarity between the experimental image and the conformally mapped pattern (figure 3(b)) is striking. Apart from a few defects, we obtain the well-known pattern of interwoven rainbows, whose periodicity is determined by the bubble volume and angle between the plates. However, the conformally mapped honeycomb is neither a true equilibrium foam structure, nor does the variation of bubble area in the experiment obey precisely that demanded from the conformal theory. We attempt to bridge the gap between the

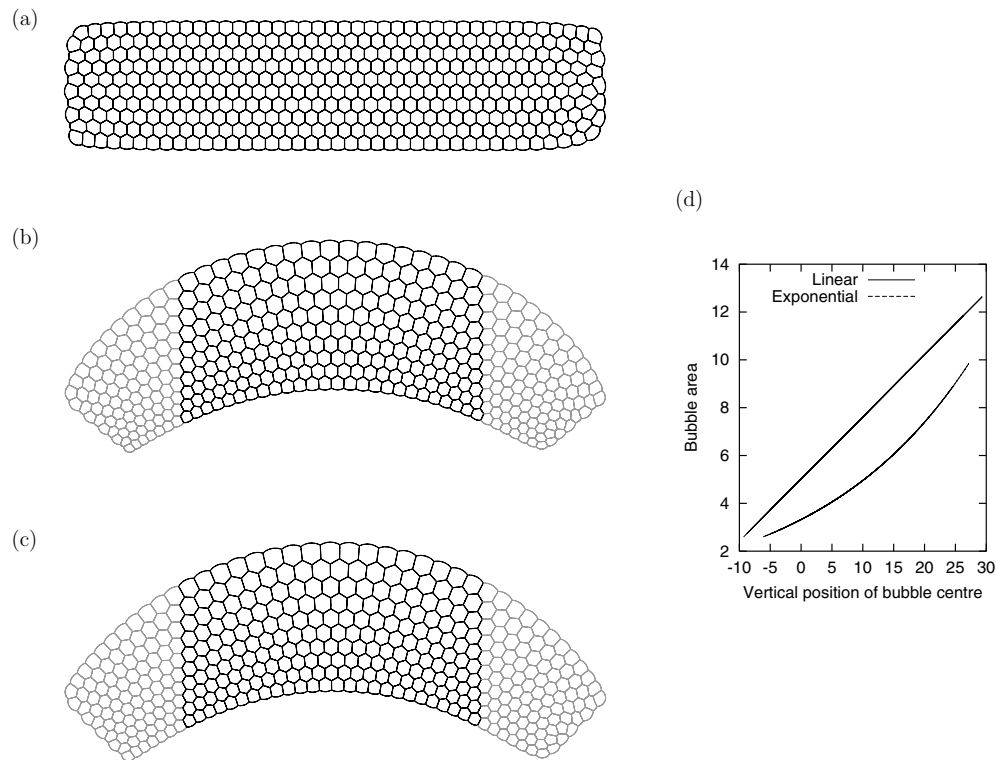


**Figure 5.** The effect of relaxation on 2D foam structures. (a) The initial rectangular configuration of 400 bubbles with equal areas (honeycomb). (b) The equilibrium structure for a linear increase in bubble area, and (c) for an exponential increase. The two are difficult to distinguish, even over a range of values of  $A(y)$ . Hence the logarithmic map is well approximated by a linear increase in the height of the experimental sample. (d) The imposed variation of area  $A$  with vertical position  $y$  for linear and exponential growth.

conformal and experimental pattern by considering the effect of relaxation on a true equilibrium structure. This may be accomplished using any of a number of published procedures (e.g., Aref and Herdtle 1990, Bolton and Weaire 1992). We have used the Surface Evolver (Brakke 1992; see the appendix) to produce the relaxed structures shown in figure 5. We begin with the equilibrated free cluster of 400 equal-area bubbles shown in figure 5(a), impose a variation of bubble area with vertical coordinate  $y$  and re-equilibrate the structure. The rectangular cluster bends to accommodate the change in cell areas, which is shown for linear and exponential  $A(y)$  in figures 5(b) and (c) respectively. This procedure introduces no topological defects, at least for a wide range of parameters in the function  $A(y)$ , in either case. Indeed, the two cases are almost indistinguishable, explaining why the linear increase in the height of the experimental system is such a good approximation to the logarithmic map. The outline of the computed sample is rather arbitrary since it is essentially the transform of the outline of the corresponding arbitrary boundary of the original monodisperse sample.

### 3.2. Conformal 2D foam with rotational symmetry

In order to generate a circle map we would need a variation of the spacing according to  $d(w) = d(r) \sim r^{-2\delta}$ . The case  $\delta = -1$  can be approximately realized by using a large

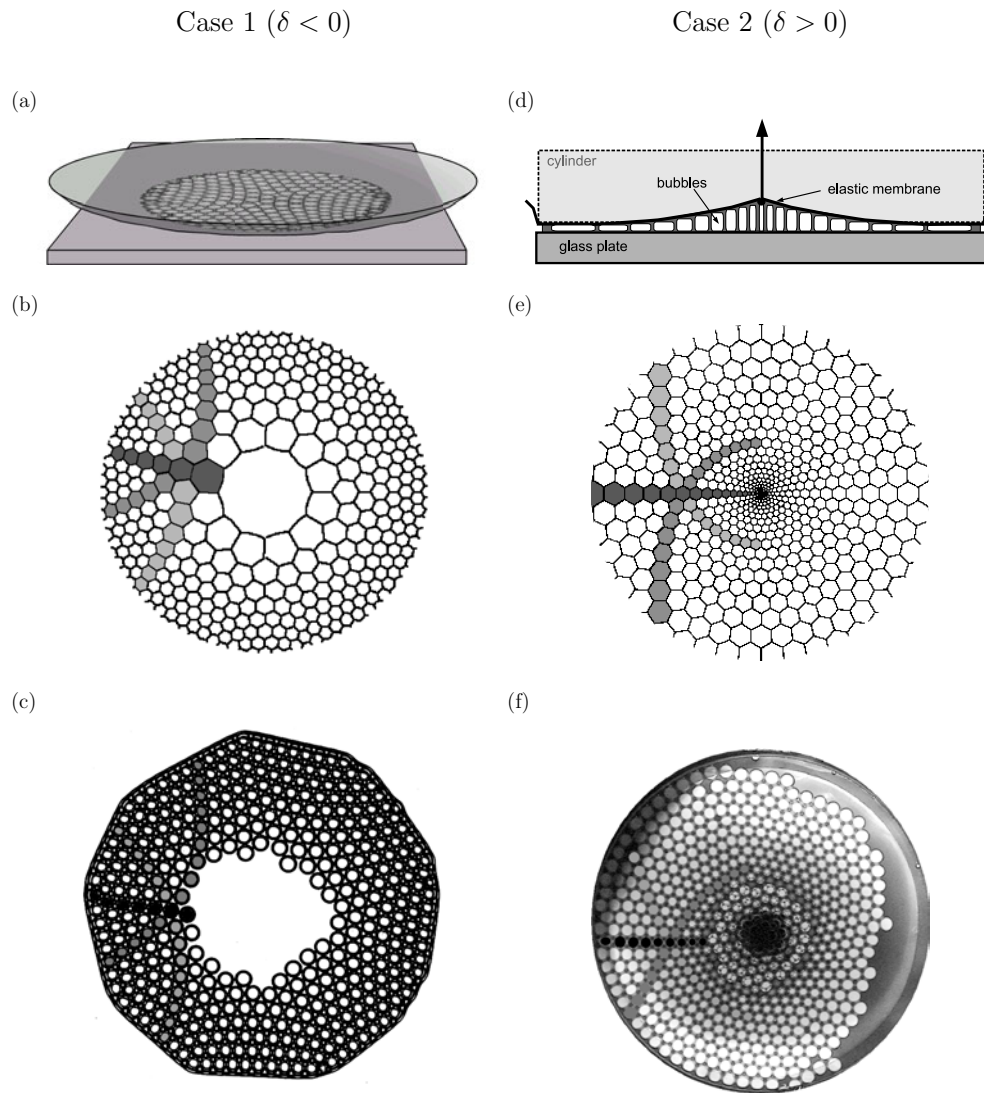


**Figure 6.** Examples for the two general cases of the circle map defined by equation (6). Case 1: decrease of bubble area with distance from centre ( $\delta < 0$ ). This can be realized experimentally by using convex vessels for the upper surface. Case 2: increase of bubble area with distance from centre ( $\delta > 0$ ), obtained between funnel-like surfaces and a glass plate. (a) A spherical vessel or watchglass can be used for an upper surface to approximate the case  $\delta = -1$ , for which (b) shows the numerical prediction, and (c) an experimental result. (d) A cross-section through the setup with which we are able to produce funnel shapes by pulling the centre of a membrane which is stretched over a cylinder. (e) Numerical example for  $\delta = 2/3$ . (f) Experimental result. The shading shows how lines of neighbouring cells that were initially straight (compare figure 1) are transformed.

spherical vessel or watch glass for the upper plate, as illustrated in figure 6(a). An experimental result can be seen in figure 6(c). Figure 6(b) shows the corresponding conformal pattern.

We do not recover the predicted 12-fold symmetry in the experiment, but obtain an almost perfect 9-fold symmetry with a few defects, whose origins will be discussed in the next section. Analysis of figure 6(c) shows that the 2D bubble area decreases almost linearly with distance

from the centre (rather than with  $r^{-2}$ , as predicted by (7)); this is more consistent with the case  $\delta = -1/2$  and 9-fold symmetry. Such discrepancies may be due to the effects of wetness and the 3D curvature of the films, as described below.

To generate cases with  $\delta > 0$  we stretch an elastic membrane across the end of a short cylinder and attach a piece of string to its centre, which is pulled to produce a ‘funnel’ shape. For an experimental result refer to figure 6(e). Comparison between theoretical prediction and experiment is more difficult here, as the patterns exhibit less symmetry and the precise shape of the funnel is not known. Nevertheless, the similarities between the patterns are obvious, with almost perfect sections being separated by lines of defects.

All the circle experiments are conducted on a glass table, as we find that the best images can be obtained with transmitted light from a diffuse source.

### 3.3. Complications and discussion

In addition to the discrepancies entailed by the approximate representation of analytic functions, a further difficulty arises if the separation increases too steeply. At a certain critical separation, bubbles with less than six sides detach from one of the surfaces to create a three-dimensional structure (Cox *et al* 2002). For the hexagonal lattice this initially affects only the bubbles on the boundary of the cluster, but the instability then propagates inwards to destroy the pattern. Even if this instability is not encountered, it should be remembered that when the two plates are not parallel, a small curvature of the films is necessary in the transverse direction. This should be taken into account in any more complete analysis.

On some occasions we have found topological defects in more or less ordered arrangements. The precise role of these defects, which might be to compensate for the approximate representation mentioned above, has not been clarified. Note that with topological arguments one can prove that any finite bubble cluster must contain at least six defects (Rivier *et al* 1984). But this theorem can be accommodated by considering the defects at the edge.

## 4. Conclusions and outlook

Two-dimensional foams offer a system for very beautiful and easily accessible experiments, which improve our understanding of foams and physically related systems. In particular, we have shown that various conformal patterns may be demonstrated. Other illuminating experiments with this simple ‘foam sandwich’ include

- coarsening, topological changes and statistics (Glazier *et al* 1987, Cox *et al* 2003),
- the structure of the beehive (Weaire and Phelan 1994),
- foam motion in various channels and networks (Drenckhan *et al* 2003).

Brakke (2002) has applied inversion in 3D (which has similar properties to the 2D case), to create three-dimensional bubble clusters, which serve to test various mathematical conjectures. In the 3D case, inversion provides a mapping between equilibrium structures only in a very limited number of cases, where surfaces are spherical.

Our technique may also be useful for the investigation of more complex patterns using more complicated surfaces or polydisperse foams. Questions also remain concerning the precise distribution and role of defects, which we sometimes find to have a periodic arrangement.

## Acknowledgments

The authors wish to thank N Rivier for advice and S Gatz for patient experimental assistance. WD was supported by the German National Merit Foundation and the Ulysses France–Ireland exchange scheme, while DW and SJC acknowledge financial assistance from the ELIPS programme of ESA.

## Appendix. Numerical procedure

To generate the computational structures in figures 3(b), 4(a) and (c), and 6(b) and (e), we use the Surface Evolver (Brakke 1992), a suite of freely available software (see [www.susqu.edu/brakke/evolver/](http://www.susqu.edu/brakke/evolver/)) that solves minimal surface problems on triangulated surfaces. Our requirements extend only as far as a 2D model, in which we take a cluster of bubbles made up of edges between pairs of vertices. We take a large finite cluster of hexagonal bubbles and apply a conformal map to the vertices of the structure.

There are a number of ways that the initial pattern of vertices and their respective edges can be obtained. The simplest is to program them directly. We prefer to construct a honeycomb lattice (for example, using a Voronoi routine in Mathematica (Wolfram Research 1999), as described by Cox and Graner (2003)) from which we can ‘cut’ the required hexagonally shaped cluster. The cutting is achieved by an Evolver routine which compares the coordinates of the centre of each bubble and eliminates those that lie outside the hexagonal region.

The map is applied to each of the vertices in turn to obtain the new structure. After moving each of the vertices, their respective edges are dragged along; by introducing many vertices along each edge (using several applications of the Evolver’s refine command, which halves the length of each edge by introducing a vertex at its centre) before mapping, we obtain an accurate picture of the mapped hexagonal structure.

Each of the conformal maps is first written in real and imaginary components. The logarithmic map (2), with  $\alpha = 1$ , becomes

$$u = \theta; \quad v = -\log|z|,$$

where  $\theta = \arg(z)$ , to give the image in figure 3(b). The circle map (6), with  $\delta = -1$ , is

$$u = \sqrt{|z|} \cos\left(\frac{1}{2}\theta\right), \quad v = \sqrt{|z|} \sin\left(\frac{1}{2}\theta\right)$$

to give figure 6(b).

## References

- Aref H and Herdtle T 1990 *Topological Fluid Mechanics* ed H Moffat and A Tsinober (Cambridge: Cambridge University Press) p 745
- Atela P, Golé C and Hotton S 2003 *Phyllotaxis, An Interactive Site for the Mathematical Study of Plant Pattern Formation* <http://www.math.smith.edu/~phylo>
- Bolton F and Weaire D 1992 The effects of Plateau borders in the two-dimensional soap froth: II. General simulation and analysis of rigidity loss transition *Phil. Mag.* **B 65** 473–87
- Bragg L and Nye J F 1947 A dynamical model of a crystal structure *Proc. R. Soc. Lond. A* **190** 474–81
- Brakke K 1992 The surface evolver *Exp. Math.* **1** 141–65
- Brakke K 2002 Private communication
- Cox S J and Graner F 2003 Large two-dimensional clusters of equal-area bubbles *Phil. Mag.* **83** 2573–84
- Cox S J, Vaz M F and Weaire D 2003 Topological changes in a two-dimensional foam cluster *Eur. Phys. J. E* **11** 29–35
- Cox S J, Weaire D and Vaz M F 2002 The transition from two-dimensional to three-dimensional foam structures *Eur. Phys. J. E* **7** 311–5
- Drenckhan W, Elias F, Hutzler S, Weaire D, Janiaud E and Bacri J C 2003 Bubble size control and measurement in the generation of ferrofluid foams *J. Appl. Phys.* **93** 10078–83

- Elias F, Bacri J-C, de Mougins F H and Spengler T 1999 Two-dimensional ferrofluid foam in an external force field: gravity arches and topological defects *Phil. Mag. Lett.* **79** 389–97
- Glazier J A, Gross S P and Stavans J 1987 Dynamics of two-dimensional soap froths *Phys. Rev. A* **36** 306–12
- Hales T C 2001 The honeycomb conjecture *Discrete Comput. Geom* **25** 1–22
- Jean R V 1984 *Mathematical Approach to Patterns and Form in Plant Growth* (New York: Wiley)
- KolosoV V Yu 1995 Nontranslation atom ordering in crystals growing in amorphous films *Aperiodic '94* ed G Chapius (Singapore: World Scientific) p 26
- Pierański P 1989 *Phase Transitions in Soft Condensed Matter (Nato Advanced Study Institute Series B: Physics vol 211)* ed T Riste and D Sherington (Dordrecht: Kluwer)
- Pittet N, Boltenhagen P, Rivier N and Weaire D 1996 Structural transitions in ordered, cylindrical foams *Europhys. Lett.* **35** 547–52
- Plateau J A F 1873 *Statique Expérimentale et Théoretique des Liquides Soumis aux Seules Forces Moléculaires* 2 vol (Paris: Gauthier-Villars)
- Prandtl L and Tietjens O G 1934 *Applied Hydro- and Aeromechanics* (New York: McGraw-Hill)
- Rivier N, Occelli R, Pantaloni J and Lissowski A 1984 Structure of Bénard convection cells, phyllotaxis and crystallography in cylindrical symmetry *J. Physique* **45** 49–63
- Rowlinson J S 2002 *Cohesion: A Scientific History of Intermolecular Forces* (Cambridge: Cambridge University Press) p 13
- Rothen F and Pierański P 1996 Mechanical equilibrium of conformal crystals *Phys. Rev. E* **53** 2828–42
- Rothen F, Pieranski P, Rivier N and Joyet A 1993 Cristaux conformes *Eur. J. Phys.* **14** 227–33
- Smith C S 1952 Grain shapes and other metallurgical applications of topology *Metal Interfaces* (Cleveland, OH: American Society for Metals) pp 65–108
- Weaire D 1999 The equilibrium structure of soap froths: inversion and decoration *Phil. Mag. Lett.* **79** 491–5
- Weaire D and Phelan R 1994 Optimal design of honeycombs *Nature* **367** 123
- Weaire D, Hutzler S and Pittet N 1992 Cylindrical packings of foam cells *Forma* **7** 259
- Weaire D and Rivier N 1984 Soap, cells and statistics—random patterns in two dimensions *Contemp. Phys.* **25** 59–99
- Wolfram Research, Inc. 1999 *Mathematica* Version 4 edition Champaign, Illinois